Bioactive Materials 37 (2024) 86–93

Contents lists available at ScienceDirect

Bioactive Materials

journal homepage: www.keaipublishing.com/en/journals/bioactive-materials

Engineering LNPs with polysarcosine lipids for mRNA delivery

Diana D. Kang [a,b,1], Xucheng Hou [a,1,**], Leiming Wang [a], Yonger Xue [a,b], Haoyuan Li [a], Yichen Zhong [a], Siyu Wang [a], Binbin Deng [c], David W. McComb [c,d], Yizhou Dong [a,b,*]

[a] Icahn Genomics Institute, Precision Immunology Institute, Department of Immunology and Immunotherapy, Department of Oncological Sciences, Tisch Cancer Institute, Friedman Brain Institute, Biomedical Engineering and Imaging Institute, Icahn School of Medicine at Mount Sinai, New York, NY, 10029, USA
[b] Division of Pharmaceutics & Pharmacology, College of Pharmacy, The Ohio State University, Columbus, OH, 43210, USA
[c] Center for Electron Microscopy and Analysis, The Ohio State University, Columbus, OH, 43212, USA
[d] Department of Materials Science and Engineering, The Ohio State University, Columbus, OH, 43210, USA

ARTICLE INFO

Keywords:
Lipid nanoparticles
mRNA
Polyethylene glycol (PEG)
Polysarcosine (pSar)

ABSTRACT

Since the approval of the lipid nanoparticles (LNP)-mRNA vaccines against the SARS-CoV-2 virus, there has been an increased interest in the delivery of mRNA through LNPs. However, current LNP formulations contain PEG lipids, which can stimulate the generation of anti-PEG antibodies. The presence of these antibodies can potentially cause adverse reactions and reduce therapeutic efficacy after administration. Given the widespread deployment of the COVID-19 vaccines, the increased exposure to PEG may necessitate the evaluation of alternative LNP formulations without PEG components. In this study, we investigated a series of polysarcosine (pSar) lipids as alternatives to the PEG lipids to determine whether pSar lipids could still provide the functionality of the PEG lipids in the ALC-0315 and SM-102 LNP systems. We found that complete replacement of the PEG lipid with a pSar lipid can increase or maintain mRNA delivery efficiency and exhibit similar safety profiles in vivo.

1. Introduction

Lipid nanoparticles (LNPs) such as ALC-0315 and SM-102 LNPs have been applied to deliver mRNAs encoding viral antigens against the SARS-CoV-2 virus [1–3]. These LNPs are typically comprised of four distinct lipid components: ionizable lipids, phospholipids, cholesterol, and polyethylene glycol lipids (PEG lipids) [4]. The main function of the PEG lipids is to stabilize and elongate the circulation time of LNPs upon administration by reducing protein binding interactions [5]. However, antibodies against the PEG lipids (anti-PEG antibodies) might arise upon repeated exposure [6]. The production of anti-PEG antibodies can potentially lead to reduced delivery efficiency of the LNPs by an accelerated blood clearance (ABC) phenomenon when the LNPs interact with the anti-PEG antibodies [7,8]. More importantly, anti-PEG antibodies have been attributed to a hypersensitivity reaction, eliciting severe allergic reactions which can potentially lead to critical anaphylaxis [7,9,10].

Before the SARS-CoV-2 pandemic, there were several reported studies to evaluate the prevalence of anti-PEG antibodies [11–13]. However, the global administration of the two LNP-mRNA vaccines triggered an increased interest in the pervasiveness of anti-PEG antibodies within the general population. Consequently, there have been numerous studies with conflicting results on the development of anti-PEG antibodies from the administration of either of the two LNP-mRNA vaccines based on different ionizable lipids. In one study, researchers found that the level of anti-PEG IgG increased after the first vaccination, but not levels of IgM or IgE [14]. In another report, the results showed that the levels of IgG did not substantially increase after each dose, but those of IgM significantly increased after the first and the third dose [15]. The role of the anti-PEG antibodies in eliciting allergic responses has also been inconsistent. Anaphylactic allergic responses to the LNP-mRNA vaccines have been reported [16–20], but the exact source of allergic reactions has been inconclusive for many cases [21–23]. Carreno and coworkers noticed different induction of anti-PEG

Peer review under responsibility of KeAi Communications Co., Ltd.
* Corresponding author. Icahn Genomics Institute, Precision Immunology Institute, Department of Immunology and Immunotherapy, Department of Oncological Sciences, Tisch Cancer Institute, Friedman Brain Institute, Biomedical Engineering and Imaging Institute, Icahn School of Medicine at Mount Sinai, New York, NY, 10029, USA.
** Corresponding author.
E-mail addresses: xucheng.hou@mssm.edu (X. Hou), yizhou.dong@mssm.edu (Y. Dong).
[1] These authors contributed equally: Diana D. Kang, Xucheng Hou.

https://doi.org/10.1016/j.bioactmat.2024.03.017
Received 27 October 2023; Received in revised form 4 March 2024; Accepted 11 March 2024

antibodies, concerning the different vaccines based on ALC-0315 or SM-102 ionizable lipids, but no evident association between anti-PEG antibodies and adverse reactions [24]. An evaluation of 20 patients with anaphylactic reactions to the LNP-mRNA vaccines found that pre-existing levels of anti-PEG IgE are not the main mechanism of anaphylactic reactions [25]. In contrast, Ju et al. reported that anti-PEG antibody levels were increased after LNP-mRNA vaccination and that the adverse systemic reactogenicity was positively correlated with increased anti-PEG antibodies after vaccination [26,27]. Another study indicated that people who displayed hypersensitivity reactions had increased levels of anti-PEG antibodies compared to people with no reactions [28]. Despite these conflicting results, an alternative lipid that can serve the functional role of PEG lipids while evading the anti-PEG antibody phenomenon can lead to the development of new types of LNP formulations.

An alternative to PEG is a polypeptoid of the amino acid sarcosine (*N*-methylated glycine) [29]. Prior studies compared the critical aggregate concentration of PEG or polysarcosine (pSar) and found that these two polymers behave similarly, which suggests that pSar can serve similar functionality as PEG for antifouling applications [30,31]. Polysarcosine has been previously investigated as a PEG substitute for therapeutic protein conjugation [32]. Other groups have investigated pSar as a surrogate to PEG by assessing its functionality to impart stealth-like properties in delivery systems such as liposomes [33–35], lipoplexes [36], and LNPs [37,38].

Here, we evaluated a panel of pSar lipids to directly replace PEG lipids in current U.S. Food and Drug Administration (FDA)-approved ALC-0315 and SM-102 based LNP formulations. We conducted characterizations and comparative analyses of the engineered LNPs and further assessed them for mRNA delivery efficiency in vitro and in vivo. We found that SM-102 based LNPs formulated with pSar lipids demonstrated comparable mRNA delivery efficiency, while ALC-0315 based LNPs formulated with pSar lipids exhibited even greater mRNA delivery efficiency compared to LNPs containing PEG lipids. Additionally, the immunogenicity profiles of the pSar LNPs are comparable to conventional PEG LNPs, validating the possibility of engineering current FDA-approved LNPs with a direct substitution of the PEG lipid with a pSar lipid.

2. Materials and methods

2.1. Materials

SM-102, ALC-0315, and ALC-0159 PEG lipids were purchased from MedKoo Biosciences. Distearoylphosphatidylcholine (DSPC), and the various polysarcosine lipids were purchased from Avanti Lipids. Cholesterol was purchased from Sigma. 1,2-dimyristoyl-rac-glycero-3-methoxypolyethylene glycol-2000 (DMG-PEG_{2000}) was purchased from Nof America. Hep3B and C2C12 cell lines were purchased from ATCC.

2.2. Lipid nanoparticles formulation

LNP-mRNA were prepared by rapid mixing of an ethanol solution containing lipids and a citrate solution containing mRNA via NanoAssemblr (Precision NanoSystems) [39]. The total flow rate was 12 mL/min at a ratio of 1:3 ethanol phase to aqueous phase. The lipid components, ionizable lipids, DSPC, cholesterol, and pSar lipids or PEG lipids were dissolved in ethanol. The lipid ratios and the mRNA to lipid mass ratio were kept consistent with published FDA-approved formulations for the respective ionizable lipids [40]. For SM-102 based LNPs, the ionizable lipid to mRNA mass ratio was 11.03, with a molar ratio of 50:10:38.5:1.5. For ALC-0315 based LNPs, the ionizable lipid to mRNA mass ratio was 14.3, with a molar ratio of 46.3:9.4:42.7:1.6. LNPs were dialyzed in 1 × PBS with Slide-A-Lyzer dialysis cassette and 0.22 μm filtered with a PES membrane filter before administration in vivo.

2.3. Lipid nanoparticles characterization

The size, polydispersity index (PDI), and zeta potential were measured by a NanoZS Zetasizer instrument (Malvern). The encapsulation efficiency was calculated by a Quant-iT™ RiboGreen assay. Briefly, LNPs were incubated with 1 × TE or 1 × TE + 1% Triton-X solution in a black 96-well plate at 37 °C for 15 min. The fluorescence intensity was measured on a BioTek Cytation 5 plate reader at excitation wavelength 485 nm and emission wavelength 528 nm.

2.4. mRNA preparation

The linear dsDNA of firefly luciferase (FLuc) and human EPO (hEPO) were obtained from Integrated DNA Technologies, which were cloned into our NASAR vector plasmid through HiFi assembly [41]. All mRNAs were synthesized by in vitro transcription, consistent with previously published protocol [41]. All mRNAs were synthesized with full *N*1-Methyl-pseudouridine substitution. The mRNAs were enzymatically capped with Vaccinia Capping Enzyme (New England Biolabs) and mRNA Cap 2′-*O*-Methyltransferase (New England Biolabs).

2.5. Luciferase assay in vitro

C2C12 cells were grown in DMEM with 10% FBS. Hep3B cells were grown in EMEM supplemented with 10% FBS. The cells were incubated at 37 °C in a 5% CO_2 environment. Cells were seeded at a density of 2 × 10^4 cells per well in a white 96-well plate, cultured overnight, and then treated with 50 ng FLuc mRNA-loaded LNPs per well. Luciferase substrate (Bright-Glo reagent, Promega) was added to each well after 18 h of incubation. After 5 min, the luminescence intensity was measured by a BioTek Cytation5 plate reader.

2.6. IVIS imaging

C57BL6 mice were used for IVIS imaging experiments. LNPs encapsulating FLuc mRNA were administered via intramuscular injection at a dose of 0.06 μg mRNA/kg/flank. 6 h after LNP administration, the mice were intraperitoneally injected with D-Luciferin substrate and were imaged on Biophotonic IVIS-Spectrum for total flux emission.

2.7. hEPO quantitation

Mouse flank muscles were isolated and frozen upon isolation. The tissue was homogenized with T-PER™ Tissue Protein Extraction Reagent (Thermo Scientific, 78510) with protease inhibitors (Thermo Scientific, 87785) at a ratio of 1 g of tissue to 10 mL of T-PER™ reagent. The sample was centrifuged at 10,000×*g* for 5 min, and the supernatant was collected for ELISA assay for hEPO quantitation (BioLegend, 442907). Mouse whole blood was collected 6 h post-injection in citrate-treated tubes. Blood was centrifuged at 1500×*g* for 10 min at 4 °C to obtain the plasma for hEPO quantitation.

2.8. Luminex analysis for cytokines and chemokines

Mouse whole blood was collected 6 h post-injection in citrate-treated tubes. Blood was centrifuged at 1500×*g* for 10 min at 4 °C to obtain the plasma. The plasma was diluted 1:1 in 1 × PBS and stored at −80 °C. Mouse cytokines and chemokines were detected by mouse cytokine/chemokine discovery assay (Eve Technologies) [42].

2.9. ELISA for anti-PEG IgG quantitation

A 96-well plate (Thermo Scientific, 456529) was coated with PEG lipid at a coating density of 2.5 μg/well overnight at 4 °C. The plate was washed 3 times with 1 × PBS, then blocked with 5% BSA in 1 × PBS for 4 h at room temperature, followed by 3 times washing with 1 × PBS.

Then, 50 × diluted plasma was added to each well, and incubated at 37 °C for 2 h. The plate was washed with 1 × PBS +0.05% Tween-20 three times, then incubated with HRP conjugated goat anti-mouse IgG antibody (Abcam, ab7068) for 1 h at 37 °C. The plate was washed with 1 × PBS +0.05% Tween-20 three times, then freshly prepared OPT substrate was added (Sigma-Aldrich, P4664). The reaction was stopped with 3 M Sulfuric Acid and read at 492 nm on a plate reader.

2.10. Animal studies

All the mouse studies were approved by the Institutional Animal Care and Use Committee at The Icahn School of Medicine at Mount Sinai (IPROTO202200000134) and complied with local, state, and federal regulations. C57BL/6J mice were ordered from Jackson Laboratories (Strain #000664).

3. Results and discussion

To investigate whether the currently used PEG lipids can be replaced with pSar lipids, we chose a panel of pSar lipids, which are shown in Fig. 1. Two distinct LNP groups were formed based on two ionizable lipids, SM-102 and ALC-0315. SM-102 based LNPs consist of SM-102, DSPC, cholesterol, and DMG-PEG_{2000}. ALC-0315 based LNPs are comprised of ALC-0315, DSPC, cholesterol, and ALC-0159 PEG lipid. The molar ratio and LNP composition were kept consistent with FDA-approved formulations [40], except for the replacement of the PEG lipid with a pSar lipid at an equivalent molar ratio. We selected pSar lipids with a repeat of 25 sarcosine moieties. This length was chosen because the resulting molecular weight of the pSar lipids is approximately 2000 g/mol, which is analogous to the molecular weight of DMG-PEG_{2000} and ALC-0159. The pSar lipids vary in the structure of the lipid chain that is linked to the pSar repeat chain (Fig. 1). C14-$pSar_{25}$ (N-Tetradecyl $pSar_{25}$), C16-$pSar_{25}$ (N-Hexadecyl $pSar_{25}$), and C18-$pSar_{25}$ (N-Octadecyl $pSar_{25}$) are comprised of a single saturated lipid tail. Other $pSar_{25}$ lipids have a double lipid tail chain. Of the double lipid tails, DOPE-$pSar_{25}$ lipid has monounsaturated lipid tails.

3.1. Characterizations of LNP properties

All LNPs were formed with a microfluidic instrument and dialyzed in 1 × PBS before characterization analyses. Upon preliminary evaluation, the hydrodynamic diameter of C14-$pSar_{25}$ lipid formulated LNPs measured greater than 500 nm. Since the size is much larger than the PEG formulations, we excluded the C14-$pSar_{25}$ lipid from further investigations. Fig. 2a shows that ALC-0315 based LNPs with single-tail lipids form bigger particles with hydrodynamic diameters greater than 200 nm. Compared to the LNPs formulated with PEG lipid, which has a diameter of approximately 85 nm, the size doubles when the LNPs were formulated with either C16-$pSar_{25}$ or C18-$pSar_{25}$ (Fig. 2a). Notably, the three other particles formulated with double lipid chained pSar lipids form smaller-sized particles. The sizes of LNPs formulated with TETAMINE-$pSar_{25}$, DMG-$pSar_{25}$, and DOPE-$pSar_{25}$ were about 150 nm, 100 nm, and 80 nm, respectively (Fig. 2a). The measured encapsulation efficiency was from 80% to 90% across all the different pSar LNPs, except ALC-0315 based LNPs with DOPE-$pSar_{25}$ (70%, Fig. 2a). The zeta potential of ALC-0315 based LNPs was mostly slightly negatively charged, except for TETAMINE-$pSar_{25}$ (Fig. 2a). For SM-102 based LNPs, the trends of sizes, PDI, and encapsulation efficiency were similar to those in ALC-0315 based LNPs (Fig. 2b). However, the zeta potential of SM-102 based LNPs were all slightly positively charged (Fig. 2b). Overall, various physicochemical properties of the LNPs formulated with pSar or PEG lipids were comparable, except for the C16-$pSar_{25}$ and C18-$pSar_{25}$ LNPs forming larger particles for both ionizable lipids.

3.2. LNPs formulated with pSar lipids for mRNA delivery in cell models

ALC-0315 and SM-102 based LNPs were formulated to be assessed in vitro across two representative cell lines: C2C12 and Hep3B cells. C2C12

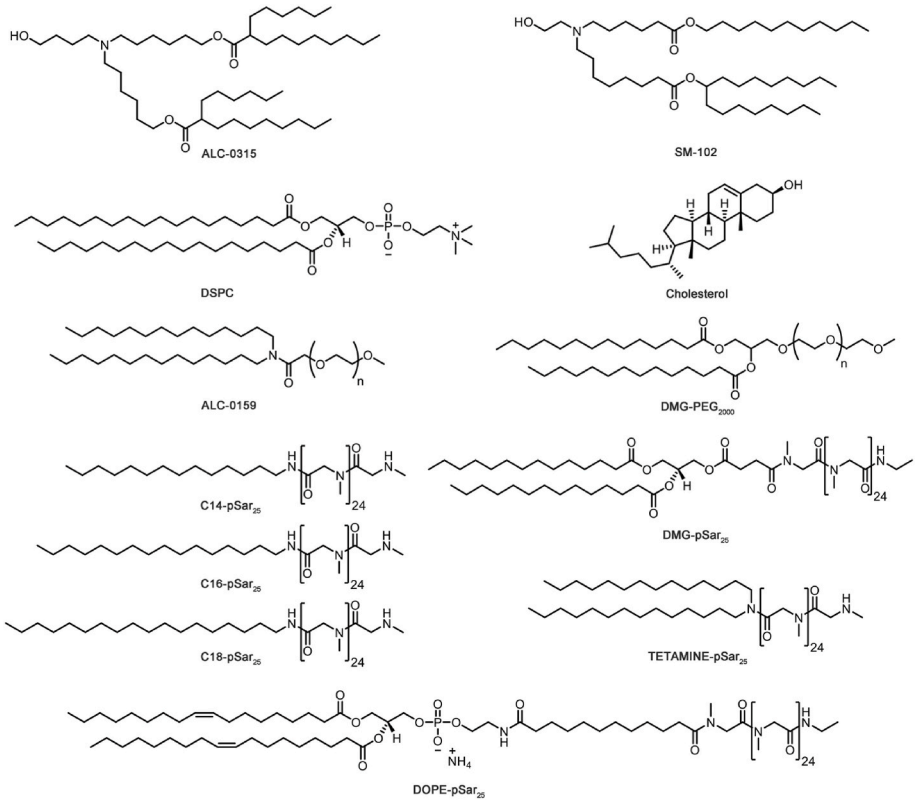

Fig. 1. Structures of ionizable lipids, DSPC, cholesterol, PEG lipids, and pSar lipids.

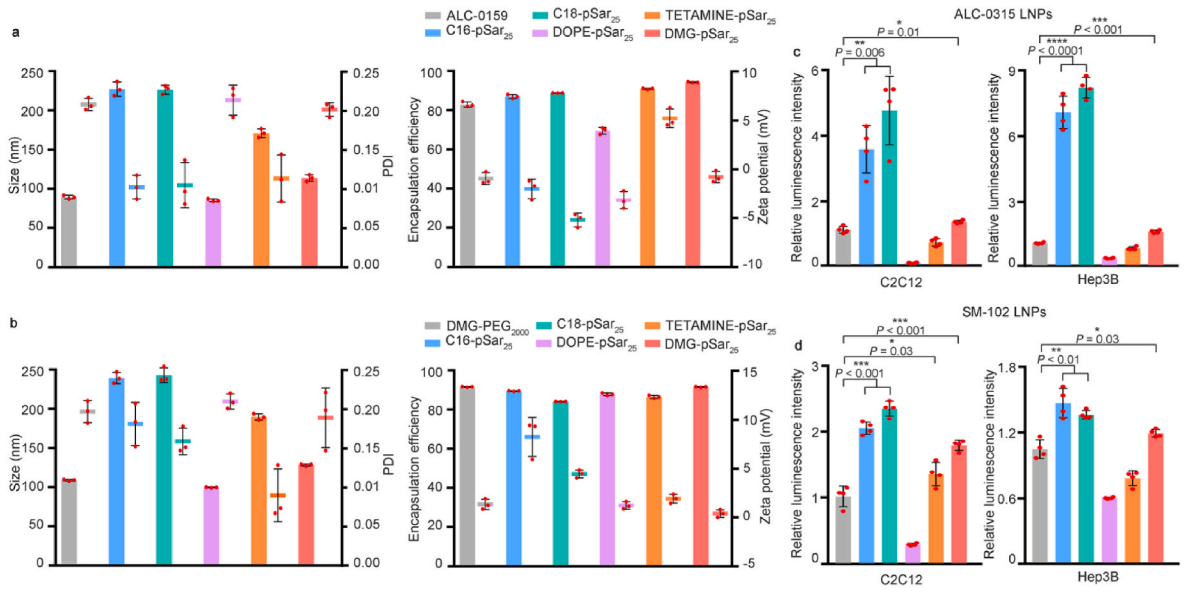

Fig. 2. Particle properties of LNPs formulated with pSar lipids and mRNA delivery in cells. a, Size, PDI, encapsulation efficiency, and zeta potential of ALC-0315 based LNPs. b, Size, PDI, encapsulation efficiency, and zeta potential of SM-102 based LNPs. c, ALC-0315 based LNPs relative luminescence intensity in C2C12 and Hep3B cells. d, SM-102 based LNPs relative luminescence intensity in C2C12 and Hep3B cells. Data in a, b, c, and d are presented as mean ± s.d. and statistical significance was analyzed by two-tailed Student's *t*-test. $^{*}P < 0.05$, $^{**}P < 0.01$, $^{***}P < 0.001$, $^{****}P < 0.0001$.

is a mouse myoblast cell line chosen to represent intramuscular administration. Hep3B is a human liver epithelial carcinoma chosen to represent the hepatic tropism of systemically administered LNPs. All LNPs were formulated with FLuc mRNA. Luminescence intensity was measured as a surrogate marker of mRNA delivery efficiency, which was normalized relative to the LNPs formulated with PEG lipid (Fig. 2c and d). Across both ionizable lipid-based particles, pSar formulated LNPs showed comparable cytotoxicity compared to PEG formulated LNPs (Supplementary Fig. 1). Furthermore, LNPs formulated with DMG-pSar$_{25}$, C16-pSar$_{25}$, C18-pSar$_{25}$, and TETAMINE-pSar$_{25}$ exhibited comparable enhanced mRNA delivery efficiency compared to the control PEG LNPs (Fig. 2c and d). For ALC-0315 based LNPs, replacing ALC-0159 PEG with DMG-PEG$_{2000}$ resulted in a decreased trend of luminescence intensity across both cell lines (Supplementary Fig. 2a), while replacing ALC-0159 PEG with DMG-pSar$_{25}$ enhanced the mRNA delivery efficiency of ALC-0315 LNPs (Fig. 2c). This result suggests that even when the same lipid structure is used, the pSar$_{25}$-lipid promotes enhanced mRNA delivery efficiency compared to the PEG lipid. To investigate the effect of the length of the pSar chain on LNP delivery efficiency, two different pSar-lipids, TETAMINE-pSar$_{35}$ and TETAMINE-pSar$_{45}$ were included and compared with TETAMINE-pSar$_{25}$. All three lipids have the same lipid tail structure, but the length of the pSar repeat is changed from 25, 35, and 45 pSar units. As shown in Supplementary Fig. 2b, SM-102 and ALC-0315 formulated with TETAMINE-pSar with different length exhibit similar particle size and PDI. Nevertheless, increasing the chain length of the pSar moiety reduced the delivery efficiency in both SM-102 and ALC-0315 based LNPs (Supplementary Fig. 2c). This is not surprising, since longer PEG lengths have also demonstrated less potent LNPs due to increased shielding effect where cellular uptake and endosomal escape is compromised [43].

Furthermore, the lipid tail structure of pSar lipids plays an essential role in mRNA delivery efficiency. For example, single lipid chained pSar lipids exhibited high mRNA delivery efficiency, especially in the ALC-0315 based LNPs. As exhibited in Fig. 2c, ALC-0315 based LNPs formulated with C18-pSar$_{25}$ lipid reached greater than a 4-fold and an 8-fold higher delivery efficiency in C2C12 and Hep3B cells, respectively. Interestingly, DOPE-pSar$_{25}$ consistently showed low mRNA delivery efficiency across both cell lines for both ionizable lipids. It was noted before that LNPs formulated with DOPE-pSar$_{25}$ and ALC-0315 lipid had the lowest mRNA encapsulation efficiency (Fig. 2a), which can potentially explain the low delivery efficiency observed in vitro for ALC-0315 based LNPs formulated with DOPE-pSar$_{25}$, but not for the SM-102 based LNPs. This suggests that even more important than the encapsulation efficiency is the ability of the LNPs to release the mRNA into the cytosol for translation. Therefore, the low delivery efficiency is more likely attributed to the difference in the saturation state of the hydrocarbon lipid tails. Previous literature states that DOPE lipid's fusogenic properties can promote the endosomal escape of the mRNA to encourage higher delivery efficiency [44–46]. Nevertheless, the conjugation of a polysarcosine chain to the DOPE lipid backbone can potentially influence the structural formation of the lipid membrane. This alteration may affect the phase behavior, particularly its ability to form inverse hexagonal phase II formation for endosomal release. Overall, in vitro results showed that direct substitution of the PEG lipids with one pSar lipid can be a viable option for LNP formulation without compromising delivery efficiency. More importantly, the different lipid chains conjugated to the pSar repeat moiety can play an important factor in the functionality of LNPs.

3.3. *LNPs formulated with pSar lipids for mRNA delivery in mice*

Taking the promising results from in vitro analysis, four pSar lipids (DMG-pSar$_{25}$, C16-pSar$_{25}$, C18-pSar$_{25}$, and TETAMINE-pSar$_{25}$) were selected to be evaluated against the control PEG LNPs in mice. ALC-0315 and SM-102 based LNPs were formulated with FLuc mRNA and were then injected intramuscularly into the flank of mice at an mRNA dose of 0.06 μg per injection. A time course evaluation of luminescence intensity in vivo showed that peak radiance is observed 6 h post intramuscular administration (Supplementary Fig. 3a). Therefore, we evaluated the delivery efficiency of the different pSar or PEG formulated LNPs at 6 h post LNPs administration. ALC-0315 based pSar LNPs resulted in statistically higher luminescence intensity than the PEG formulated LNPs (Fig. 3a, Supplementary Fig. 3b). LNPs formulated with C16-pSar$_{25}$ and DMG-pSar$_{25}$ generated greater than 5-fold higher total flux compared to PEG LNPs. On the other hand, the average luminescence intensity for the SM-102 based pSar LNPs was similar to that for the PEG LNPs (Fig. 3b, Supplementary Fig. 3b). To further examine the LNPs formulated with pSar lipids in vivo, we synthesized mRNA encoding for human

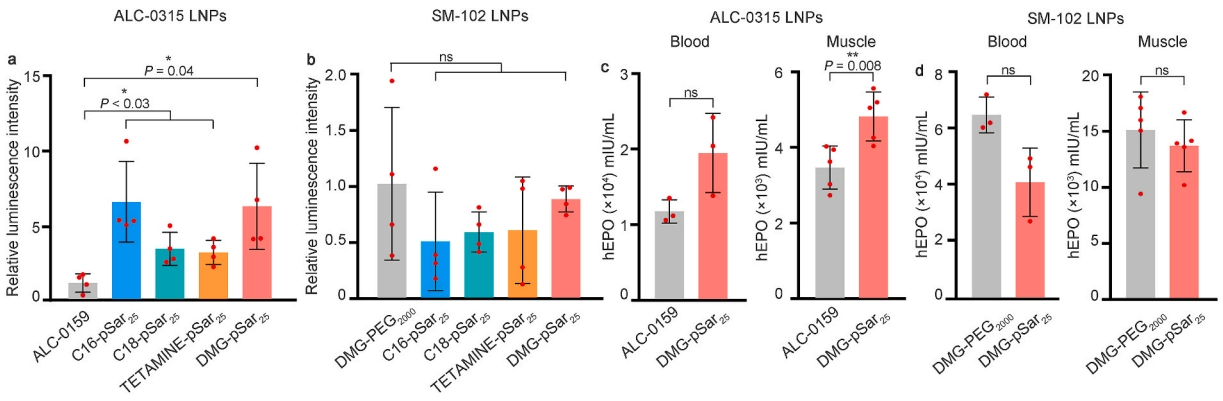

Fig. 3. In vivo administration of pSar and PEG LNPs. a, IVIS measurement of ALC-0315 based LNPs. b, IVIS measurement of SM-102 based LNPs. c, human EPO quantitation of ALC-0315 based LNPs in the blood and muscle. d, human EPO quantitation of SM-102 based LNPs in the blood and muscle. All data are presented as mean ± s.d. and statistical significance was analyzed by two-tailed Student's *t*-test. $*P < 0.05$, $**P < 0.01$, ns, no significance.

erythropoietin (hEPO), a therapeutically relevant cargo. In the following study, we narrowed down the pSar lipid to DMG-pSar$_{25}$ based on results from cellular data, LNPs characterization, and in vivo IVIS data. Since DMG-pSar$_{25}$ has the same lipid backbone as DMG-PEG$_{2000}$, and shares similar 14-carbon lipid tails with ALC-0159, the differential mRNA delivery efficiency could reflect the effects of the PEG or pSar chains, rather than the lipid backbone. Six hours post intramuscular injection, the mice were euthanized, and the flank muscle and blood were collected for hEPO quantitation through ELISA. ALC-0315 based LNPs formulated with DMG-pSar$_{25}$ resulted in significantly higher levels of hEPO in the muscle compared to ALC-0159 PEG LNPs (Fig. 3c), which confirms the enhanced mRNA delivery efficiency as measured through luminescence intensity. SM-102 based LNPs showed similar results in that pSar LNPs and PEG LNPs led to the comparable translation of the hEPO protein (Fig. 3d). The in vivo results from these two mRNAs provide valuable insights into the role of different lipid components within the LNP system in mediating mRNA delivery efficiency. Interestingly, the results vary slightly between the different ionizable lipids. For ALC-0315 based LNPs, replacement of the PEG lipid with DMG-pSar$_{25}$ lipid increases the expression of the encoded mRNA, thereby indicating enhanced delivery efficiency. The statistically significant higher expression across both mRNAs supports this finding. On the other hand, SM-102 based LNPs did not show a statistically significant increase in mRNA delivery efficiency between DMG-pSar$_{25}$ and DMG-PEG$_{2000}$ LNPs. Taken together, although direct replacement of pSar lipid can maintain similar or even enhance the mRNA delivery efficiency when compared to current PEG LNPs, more focused evaluations based on specific ionizable lipids and other lipid components must be addressed to further confirm and validate an alternative PEG-free LNP system.

3.4. Comparison of LNPs immunogenicity in vivo

The main functional role of LNPs is to mediate mRNA delivery for expression. However, LNPs itself can elicit immunogenic responses, which can affect the overall innate immune responses to the LNPs administration. Therefore, we evaluated cytokine and chemokine induction profiles of pSar and PEG LNPs. The blood from the mice either injected with DMG-pSar$_{25}$ or PEG LNPs were collected 6 h post-administration and analyzed for a broad panel cytokine and chemokine analysis with a Luminex Assay. The expression profiles for the 32 different cytokines and chemokines were similar regardless of LNPs formulated with pSar or PEG lipids (Fig. 4a). For instance, CXCL10, an interferon-γ induced chemokine, increased approximately 5-fold for both pSar and PEG LNPs treated mice, indicating the activation of the innate immune system. Similarly, the upregulation of CXCL10 was also observed in patients administered with the BNT162b2 mRNA vaccine, which is a marker of active humoral immunity following vaccination [47]. Additionally, the level of IL-6 increased dramatically, close to 10-fold, regardless of pSar or PEG LNPs. IL-6 is known to induce a robust T follicular helper dependent germinal center B cell response, crucial for effective antibody responses [48]. Interestingly, some cytokines or chemokines showed differential expressions between PEG and pSar LNPs (Fig. 4b and c). For example, SM-102 based LNPs formulated with DMG-pSar$_{25}$ lipid show higher expression of cytokines or chemokines such as G-CSF, IL-6, and CXCL1 compared to the PEG counterpart (Fig. 4b). Recent clinical findings indicate that the heightened levels of G-CSF and CXCL1 may stem from the adjuvant effect of a vaccine [49]. Moreover, the upregulation of G-CSF, IL-6, and CXCL1 was observed in another study where mice were treated with an LNP-mRNA vaccine [50]. The increase in these signaling molecules is potentially attributed to the presence of the ionizable lipid [50]. Additionally, the length of the PEG chain can affect the immunogenicity of PEG lipids [51]. For example, a low-molecular-weight PEG$_{200\text{-}400}$ may suppress the generation of pro-inflammatory cytokines such as IL-6 [52]. Thus, utilizing PEG$_{200\text{-}400}$ can be potentially beneficial to reduce immunogenic responses to the LNPs. Nonetheless, PEG$_{2000}$ is used in several FDA-approved liposome- and LNP-based drugs [53]. This may be because PEG$_{2000}$ can balance the functional roles of abating protein adsorption while maintaining delivery efficiency [43,54,55].

As previously noted, lipid components can trigger different immunogenic responses. Comparing SM-102 and ALC-0315 based LNPs both formulated with DMG-pSar$_{25}$, some cytokines or chemokines were higher for SM-102 based LNPs whereas some levels were lower (Fig. 4d). The difference in the upregulation of specific cytokines across SM-102 and ALC-0315 based LNPs suggests that the overall LNPs composition is critical for eliciting different immunogenic responses. This reflects the important role of ionizable lipids in the overall immunogenicity of LNPs [56,57]. With an increased interest in implementing LNPs for various vaccine and therapeutic applications [58–62], more focused investigations on the efficacy and safety of the complete LNP formulation are necessary for clinical advancements. Thus, the replacement of pSar lipid should be evaluated in the context of the specific ionizable lipid and the complete LNP formulation to assess the overall interactive effects of the LNP system in eliciting an immune response. Capturing the immune stimulatory effects of the LNP system can be especially advantageous for certain indications, such as vaccines, which may benefit from activated humoral and cellular immunity [63].

To further compare the immunogenicity of pSar or PEG formulated LNPs, we assessed whether a repeat administration of LNPs will elicit a heightened immune response by analyzing the systemic cytokine release profiles. The repeated injection elicited a pro-inflammatory pattern that was similar to the first-time administration (Fig. 4a, Supplementary Fig. 4a). The levels of total circulating IgG were slightly elevated in mice

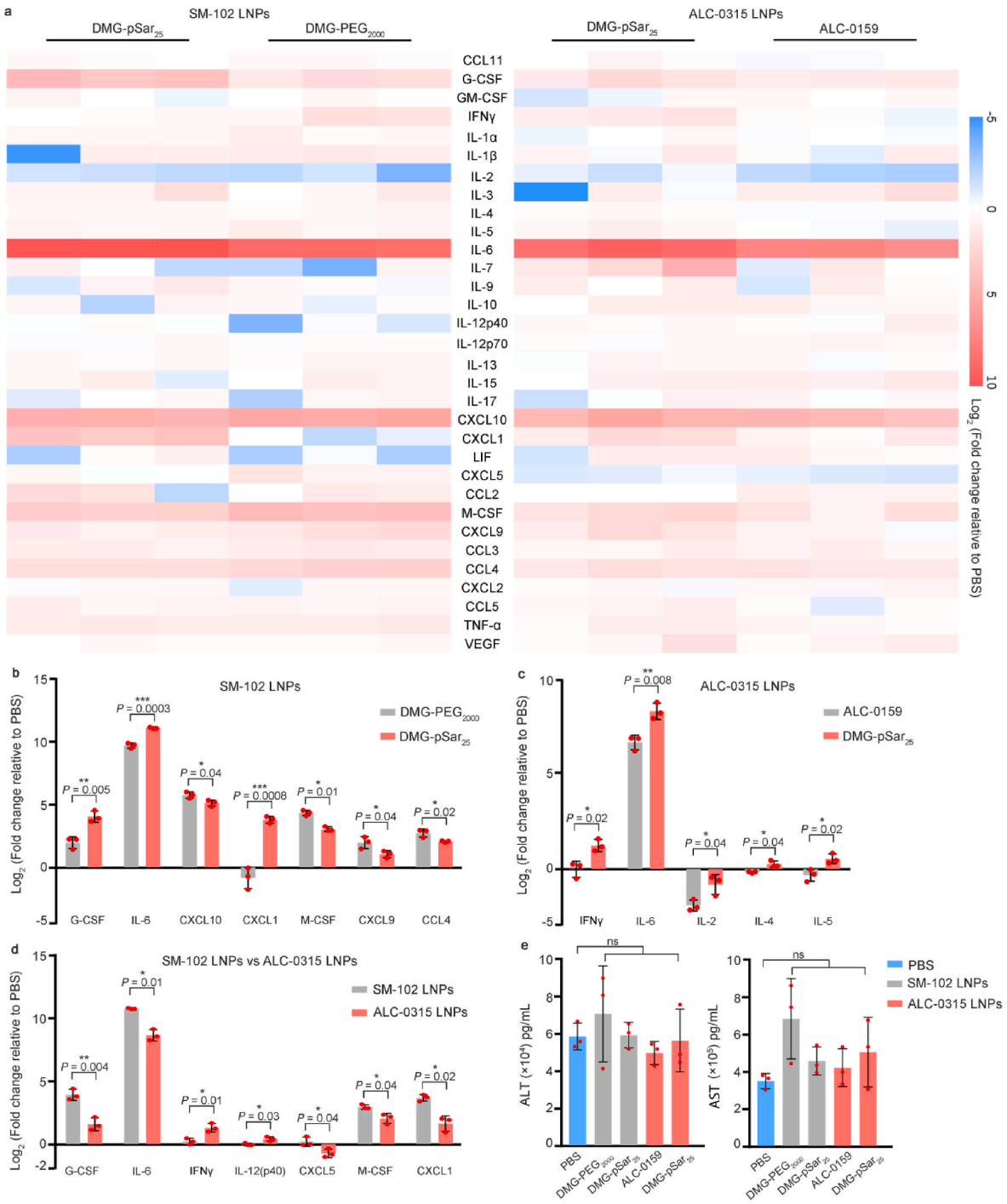

Fig. 4. Systemic immunogenicity and safety evaluation. a, Heatmap showing log fold change compared to PBS-treated mice for 32 different cytokines and chemokines. b, SM-102 based LNPs, comparison between DMG-pSar$_{25}$ and DMG-PEG$_{2000}$ LNPs. c, ALC-0315 based LNPs, comparison between DMG-pSar$_{25}$ and ALC-0159 LNPs. d, Comparison of relative cytokine and chemokine expression of DMG-pSar$_{25}$ formulated with SM-102 or ALC-0315. e, ALT and AST quantitation. Data in b to e are presented as mean ± s.d. and statistical significance was analyzed by two-tailed Student's *t*-test. $^{*}P < 0.05$, $^{**}P < 0.01$, $^{***}P < 0.001$, ns, no significance.

that received either pSar or PEG formulated LNPs compared to untreated mice but were statistically insignificant (Supplementary Fig. 4b). Additionally, we performed an ELISA to detect anti-PEG mouse IgG after the second time administration. The results showed that pSar LNP treated mice did not induce the production of antibodies against PEG, whereas PEG LNP injected mice showed a heightened O.D. signal, indicating the presence of anti-PEG antibodies (Supplementary Fig. 4c). Therefore, administration of pSar LNPs will not react with existing anti-PEG antibodies. This ELISA study is similar to the method reported previously that assessed the production of antibodies against PEG in a liposome format [35]. According to this study, pSar formulated liposomes induced lower levels of antibodies than PEG formulated liposomes [35]. Taken together, the replacement of PEG lipids with a pSar lipid in current FDA-approved LNP formulations based on ALC-0315 and SM-102 can achieve functional mRNA delivery while potentially evading concerns regarding existing anti-PEG antibodies. Lastly, we assessed for hepatic toxicity by quantifying the levels of aspartate transaminase (AST) and alanine transaminase (ALT) in the plasma. The

levels of AST and ALT were quantified from mouse plasma obtained 6 h after intramuscular injection of either LNPs containing pSar lipid or PEG lipid. Compared to the PBS-treated mouse, administration of both ALC-0315 or SM-102 based LNPs formulated with pSar or PEG lipids showed no significant increase in both enzymes, which suggests that the liver function was not compromised after the single administration (Fig. 4e).

4. Conclusion

In this study, we observed that the complete substitution of a PEG lipid with a pSar lipid can form LNPs with comparable physicochemical properties and maintain or even enhance mRNA delivery efficiency in vitro and in vivo across two different FDA-approved ionizable lipid-based formulations (SM-102 and ALC-0315). This is potentially a valuable PEG-free alternative system that can be used for localized injections, such as intramuscular vaccine injections or intratumoral therapeutic applications. With the increased number of pharmaceutical products with PEG, the clinical impact of anti-PEG antibodies and PEG immunogenicity needs to be considered for the future development of novel pharmaceutical products. Immunosafety is vital for further development and applications of LNPs, therefore circumventing adverse immune reactions can present a valuable translational application. Although a direct replacement of PEG lipid with a pSar lipid can expedite the development and validation of new LNP formulations, further studies designed to optimize the LNP formulations with respect to the specific ionizable lipid and pSar lipid can potentially increase the delivery efficiency and fine-tune the overall immunogenicity of the LNPs. Overall, LNPs with pSar lipids represent a promising platform of PEG-free LNPs for mRNA delivery, which merits a comprehensive development for future vaccines and therapeutic applications.

Ethics approval

All the mouse studies were approved by the Institutional Animal Care and Use Committee at The Icahn School of Medicine at Mount Sinai (IPROTO202200000134), and complied with local, state, and federal regulations.

CRediT authorship contribution statement

Diana D. Kang: Writing – review & editing, Writing – original draft, Methodology, Formal analysis, Data curation, Conceptualization. **Xucheng Hou:** Writing – review & editing, Writing – original draft, Methodology, Formal analysis, Data curation, Conceptualization. **Leiming Wang:** Writing – review & editing, Visualization. **Yonger Xue:** Writing – review & editing, Data curation. **Haoyuan Li:** Data curation. **Yichen Zhong:** Writing – review & editing, Data curation. **Siyu Wang:** Data curation. **Binbin Deng:** Data curation. **David W. McComb:** Data curation. **Yizhou Dong:** Writing – review & editing, Supervision, Funding acquisition, Conceptualization.

Declaration of competing interest

Y.D. is a scientific advisory board member and holds equity in Arbor Biotechnologies and Sirnagen Therapeutics. Y.D. is a co-founder and holds equity in Immunanoengineering Therapeutics. Other authors declare no conflict of interest.

Acknowledgments

D.D.K and X.H. contributed equally to this work. The authors acknowledge the use of the core facility provided by the Tisch Cancer Institute and BioMedical Engineering and Imaging Institute at the Icahn School of Medicine at Mount Sinai. Electron microscopy was performed at the Center for Electron Microscopy and Analysis (CEMAS) at The Ohio State University. Authors acknowledge the usage of BioRender to generate certain figures. Y.D. acknowledges the support from the Icahn School of Medicine at Mount Sinai.

Appendix A. Supplementary data

Supplementary data to this article can be found online at https://doi.org/10.1016/j.bioactmat.2024.03.017.

References

[1] F.P. Polack, et al., Safety and efficacy of the BNT162b2 mRNA covid-19 vaccine, N. Engl. J. Med. 383 (2020) 2603–2615, https://doi.org/10.1056/NEJMoa2034577.
[2] L.R. Baden, et al., Efficacy and safety of the mRNA-1273 SARS-CoV-2 vaccine, N. Engl. J. Med. 384 (2021) 403–416, https://doi.org/10.1056/NEJMoa2035389.
[3] A. Hussain, et al., mRNA vaccines for COVID-19 and diverse diseases, J. Contr. Release 345 (2022) 314–333, https://doi.org/10.1016/j.jconrel.2022.03.032.
[4] X. Hou, T. Zaks, R. Langer, Y. Dong, Lipid nanoparticles for mRNA delivery, Nat. Rev. Mater. 1–17 (2021), https://doi.org/10.1038/s41578-021-00358-0.
[5] Y. Eygeris, M. Gupta, J. Kim, G. Sahay, Chemistry of lipid nanoparticles for RNA delivery, Acc. Chem. Res. 55 (2022) 2–12, https://doi.org/10.1021/acs.accounts.1c00544.
[6] X. Wang, T. Ishida, H. Kiwada, Anti-PEG IgM elicited by injection of liposomes is involved in the enhanced blood clearance of a subsequent dose of PEGylated liposomes, J. Contr. Release 119 (2007) 236–244, https://doi.org/10.1016/j.jconrel.2007.02.010.
[7] G.T. Kozma, T. Shimizu, T. Ishida, J. Szebeni, Anti-PEG antibodies: properties, formation, testing and role in adverse immune reactions to PEGylated nano-biopharmaceuticals, Adv. Drug Deliv. Rev. 154–155 (2020) 163–175, https://doi.org/10.1016/j.addr.2020.07.024.
[8] D. Shi, et al., To PEGylate or not to PEGylate: immunological properties of nanomedicine's most popular component, polyethylene glycol and its alternatives, Adv. Drug Deliv. Rev. 180 (2022) 114079, https://doi.org/10.1016/j.addr.2021.114079.
[9] P. Zhang, F. Sun, S. Liu, S. Jiang, Anti-PEG antibodies in the clinic: current issues and beyond PEGylation, J. Contr. Release 244 (2016) 184–193, https://doi.org/10.1016/j.jconrel.2016.06.040.
[10] R. Tenchov, J.M. Sasso, Q.A. Zhou, PEGylated lipid nanoparticle formulations: immunological safety and efficiency perspective, Bioconjugate Chem. 34 (2023) 941–960, https://doi.org/10.1021/acs.bioconjchem.3c00174.
[11] B.M. Chen, et al., Measurement of pre-existing IgG and IgM antibodies against polyethylene glycol in healthy individuals, Anal. Chem. 88 (2016) 10661–10666, https://doi.org/10.1021/acs.analchem.6b03109.
[12] Q. Yang, et al., Analysis of pre-existing IgG and IgM antibodies against polyethylene glycol (PEG) in the general population, Anal. Chem. 88 (2016) 11804–11812, https://doi.org/10.1021/acs.analchem.6b03437.
[13] C. Lubich, et al., The mystery of antibodies against polyethylene glycol (PEG) - what do we know? Pharm. Res. (N. Y.) 33 (2016) 2239–2249, https://doi.org/10.1007/s11095-016-1961-x.
[14] Y. Bavli, et al., Anti-PEG antibodies before and after a first dose of Comirnaty(R) (mRNA-LNP-based SARS-CoV-2 vaccine), J. Contr. Release 354 (2023) 316–322, https://doi.org/10.1016/j.jconrel.2022.12.039.
[15] G. Guerrini, et al., Monitoring anti-PEG antibodies level upon repeated lipid nanoparticle-based COVID-19 vaccine administration, Int. J. Mol. Sci. 23 (2022), https://doi.org/10.3390/ijms23168838.
[16] R. Rubin, Allergic reactions to mRNA vaccines, JAMA 325 (2021) 2038, https://doi.org/10.1001/jama.2021.6941.
[17] K.G. Blumenthal, et al., Acute allergic reactions to mRNA COVID-19 vaccines, JAMA 325 (2021) 1562–1565, https://doi.org/10.1001/jama.2021.3976.
[18] L. Nilsson, A. Csuth, J. Storsaeter, L.H. Garvey, M.C. Jenmalm, Vaccine allergy: evidence to consider for COVID-19 vaccines, Curr. Opin. Allergy Clin. Immunol. 21 (2021) 401–409, https://doi.org/10.1097/ACI.0000000000000762.
[19] B. Cabanillas, N. Novak, Allergy to COVID-19 vaccines: a current update, Allergol. Int. 70 (2021) 313–318, https://doi.org/10.1016/j.alit.2021.04.003.
[20] M.D. McSweeney, M. Mohan, S.P. Commins, S.K. Lai, Anaphylaxis to pfizer/BioNTech mRNA COVID-19 vaccine in a patient with clinically confirmed PEG allergy, Front Allergy 2 (2021) 715844, https://doi.org/10.3389/falgy.2021.715844.
[21] P. Bigini, et al., The role and impact of polyethylene glycol on anaphylactic reactions to COVID-19 nano-vaccines, Nat. Nanotechnol. 16 (2021) 1169–1171, https://doi.org/10.1038/s41565-021-01001-3.
[22] P. Sellaturay, S. Nasser, S. Islam, P. Gurugama, P.W. Ewan, Polyethylene glycol (PEG) is a cause of anaphylaxis to the Pfizer/BioNTech mRNA COVID-19 vaccine, Clin. Exp. Allergy 51 (2021) 861–863, https://doi.org/10.1111/cea.13874.
[23] K.A. Risma, et al., Potential mechanisms of anaphylaxis to COVID-19 mRNA vaccines, J. Allergy Clin. Immunol. 147 (2021) 2075–2082 e2072, https://doi.org/10.1016/j.jaci.2021.04.002.
[24] J.M. Carreno, et al., mRNA-1273 but not BNT162b2 induces antibodies against polyethylene glycol (PEG) contained in mRNA-based vaccine formulations, Vaccine 40 (2022) 6114–6124, https://doi.org/10.1016/j.vaccine.2022.08.024.

[25] Z.H. Zhou, et al., Evaluation of association of anti-PEG antibodies with anaphylaxis after mRNA COVID-19 vaccination, Vaccine 41 (2023) 4183–4189, https://doi.org/10.1016/j.vaccine.2023.05.029.
[26] Y. Ju, et al., Impact of anti-PEG antibodies induced by SARS-CoV-2 mRNA vaccines, Nat. Rev. Immunol. 23 (2023) 135–136, https://doi.org/10.1038/s41577-022-00825-x.
[27] Y. Ju, et al., Anti-PEG antibodies boosted in humans by SARS-CoV-2 lipid nanoparticle mRNA vaccine, ACS Nano 16 (2022) 11769–11780, https://doi.org/10.1021/acsnano.2c04543.
[28] G.T. Kozma, et al., Role of anti-polyethylene glycol (PEG) antibodies in the allergic reactions to PEG-containing Covid-19 vaccines: evidence for immunogenicity of PEG, Vaccine 41 (2023) 4561–4570, https://doi.org/10.1016/j.vaccine.2023.06.009.
[29] A. Birke, J. Ling, M. Barz, Polysarcosine-containing copolymers: synthesis, characterization, self-assembly, and applications, Prog. Polym. Sci. 81 (2018) 163–208, https://doi.org/10.1016/j.progpolymsci.2018.01.002.
[30] D. Huesmann, A. Sevenich, B. Weber, M. Barz, A head-to-head comparison of poly (sarcosine) and poly(ethylene glycol) in peptidic, amphiphilic block copolymers, Polymer 67 (2015) 240–248, https://doi.org/10.1016/j.polymer.2015.04.070.
[31] K.H. Lau, et al., Surface-grafted polysarcosine as a peptoid antifouling polymer brush, Langmuir 28 (2012) 16099–16107, https://doi.org/10.1021/la302131n.
[32] Y. Hu, Y. Hou, H. Wang, H. Lu, Polysarcosine as an alternative to PEG for therapeutic protein conjugation, Bioconjugate Chem. 29 (2018) 2232–2238, https://doi.org/10.1021/acs.bioconjchem.8b00237.
[33] S. Bleher, et al., Poly(Sarcosine) surface modification imparts stealth-like properties to liposomes, Small 15 (2019) e1904716, https://doi.org/10.1002/smll.201904716.
[34] B. Weber, et al., Polysarcosine-based lipids: from lipopolypeptoid micelles to stealth-like lipids in Langmuir blodgett monolayers, Polymers 8 (2016), https://doi.org/10.3390/polym8120427.
[35] K. Son, et al., Evasion of the accelerated blood clearance phenomenon by polysarcosine coating of liposomes, J. Contr. Release 322 (2020) 209–216, https://doi.org/10.1016/j.jconrel.2020.03.022.
[36] D. Bi, et al., Polysarcosine-based lipid formulations for intracranial delivery of mRNA, J. Contr. Release 356 (2023) 1–13, https://doi.org/10.1016/j.jconrel.2023.02.021.
[37] S.S. Nogueira, et al., Polysarcosine-functionalized lipid nanoparticles for therapeutic mRNA delivery, ACS Appl. Nano Mater. 3 (2020) 10634–10645, https://doi.org/10.1021/acsanm.0c01834.
[38] C. Wilhelmy, et al., Polysarcosine-functionalized mRNA lipid nanoparticles tailored for immunotherapy, Pharmaceutics 15 (2023).
[39] W. Li, et al., Biomimetic nanoparticles deliver mRNAs encoding costimulatory receptors and enhance T cell mediated cancer immunotherapy, Nat. Commun. 12 (2021) 7264, https://doi.org/10.1038/s41467-021-27434-x.
[40] L. Schoenmaker, et al., mRNA-lipid nanoparticle COVID-19 vaccines: structure and stability, Int. J. Pharm. 601 (2021) 120586, https://doi.org/10.1016/j.ijpharm.2021.120586.
[41] C. Zeng, et al., Leveraging mRNA sequences and nanoparticles to deliver SARS-CoV-2 antigens in vivo, Adv. Mater. 32 (2020) e2004452, https://doi.org/10.1002/adma.202004452.
[42] Y. Zhang, et al., Close the cancer-immunity cycle by integrating lipid nanoparticle-mRNA formulations and dendritic cell therapy, Nat. Nanotechnol. (2023), https://doi.org/10.1038/s41565-023-01453-9.
[43] D. Pozzi, et al., Effect of polyethyleneglycol (PEG) chain length on the bio-nano-interactions between PEGylated lipid nanoparticles and biological fluids: from nanostructure to uptake in cancer cells, Nanoscale 6 (2014) 2782–2792, https://doi.org/10.1039/c3nr05559k.
[44] X. Cheng, R.J. Lee, The role of helper lipids in lipid nanoparticles (LNPs) designed for oligonucleotide delivery, Adv. Drug Deliv. Rev. 99 (2016) 129–137, https://doi.org/10.1016/j.addr.2016.01.022.
[45] D.C. Litzinger, L. Huang, Phosphatidylethanolamine liposomes: drug delivery, gene transfer and immunodiagnostic applications, Biochim. Biophys. Acta 1113 (1992) 201–227, https://doi.org/10.1016/0304-4157(92)90039-d.
[46] I.S. Zuhorn, et al., Nonbilayer phase of lipoplex-membrane mixture determines endosomal escape of genetic cargo and transfection efficiency, Mol. Ther. 11 (2005) 801–810, https://doi.org/10.1016/j.ymthe.2004.12.018.
[47] C. Bergamaschi, et al., Systemic IL-15, IFN-gamma, and IP-10/CXCL10 signature associated with effective immune response to SARS-CoV-2 in BNT162b2 mRNA vaccine recipients, Cell Rep. 36 (2021) 109504, https://doi.org/10.1016/j.celrep.2021.109504.
[48] S.T. Crotty, Follicular helper cell differentiation, function, and roles in disease, Immunity 41 (2014) 529–542, https://doi.org/10.1016/j.immuni.2014.10.004.
[49] B. Pulendran, S.A. P, D.T. O'Hagan, Emerging concepts in the science of vaccine adjuvants, Nat. Rev. Drug Discov. 20 (2021) 454–475, https://doi.org/10.1038/s41573-021-00163-y.
[50] M.G. Alameh, et al., Lipid nanoparticles enhance the efficacy of mRNA and protein subunit vaccines by inducing robust T follicular helper cell and humoral responses, Immunity 54 (2021) 2877–2892 e2877, https://doi.org/10.1016/j.immuni.2021.11.001.
[51] E. Wenande, L.H. Garvey, Immediate-type hypersensitivity to polyethylene glycols: a review, Clin. Exp. Allergy 46 (2016) 907–922, https://doi.org/10.1111/cea.12760.
[52] G.L. Ackland, et al., Low-molecular-weight polyethylene glycol improves survival in experimental sepsis, Crit. Care Med. 38 (2010) 629–636, https://doi.org/10.1097/CCM.0b013e3181c8fcd0.
[53] Y. Gao, M. Joshi, Z. Zhao, S. Mitragotri, PEGylated therapeutics in the clinic, Bioeng Transl Med 9 (2024) e10600, https://doi.org/10.1002/btm2.10600.
[54] H. Lee, R.G. Larson, Adsorption of plasma proteins onto PEGylated lipid bilayers: the effect of PEG size and grafting density, Biomacromolecules 17 (2016) 1757–1765, https://doi.org/10.1021/acs.biomac.6b00146.
[55] M. Berger, et al., Effect of PEG anchor and serum on lipid nanoparticles: development of a nanoparticles tracking method, Pharmaceutics 15 (2023), https://doi.org/10.3390/pharmaceutics15020597.
[56] C. Hald Albertsen, et al., The role of lipid components in lipid nanoparticles for vaccines and gene therapy, Adv. Drug Deliv. Rev. 188 (2022) 114416, https://doi.org/10.1016/j.addr.2022.114416.
[57] B. Li, et al., Enhancing the immunogenicity of lipid-nanoparticle mRNA vaccines by adjuvanting the ionizable lipid and the mRNA, Nat. Biomed. Eng. (2023), https://doi.org/10.1038/s41551-023-01082-6.
[58] J. Nguyen, F.C. Szoka, Nucleic acid delivery: the missing pieces of the puzzle? Acc. Chem. Res. 45 (2012) 1153–1162, https://doi.org/10.1021/ar3000162.
[59] J.A. Kulkarni, P.R. Cullis, R. van der Meel, Lipid nanoparticles enabling gene therapies: from concepts to clinical utility, Nucleic Acid Therapeut. 28 (2018) 146–157, https://doi.org/10.1089/nat.2018.0721.
[60] J. Chen, et al., Lipid nanoparticle-mediated lymph node-targeting delivery of mRNA cancer vaccine elicits robust CD8(+) T cell response, Proc. Natl. Acad. Sci. U. S. A. 119 (2022) e2207841119, https://doi.org/10.1073/pnas.2207841119.
[61] Z. Cui, et al., Cas13d knockdown of lung protease Ctsl prevents and treats SARS-CoV-2 infection, Nat. Chem. Biol. 18 (2022) 1056–1064, https://doi.org/10.1038/s41589-022-01094-4.
[62] J.Q. Liu, et al., Intratumoral delivery of IL-12 and IL-27 mRNA using lipid nanoparticles for cancer immunotherapy, J. Contr. Release 345 (2022) 306–313, https://doi.org/10.1016/j.jconrel.2022.03.021.
[63] Y. Lee, M. Jeong, J. Park, H. Jung, H. Lee, Immunogenicity of lipid nanoparticles and its impact on the efficacy of mRNA vaccines and therapeutics, Exp. Mol. Med. (2023), https://doi.org/10.1038/s12276-023-01086-x.